INELASTIC SCATTERING OF 6.6-MeV PROTONS ON Ca^{40} AND Mn^{55}

S. S. VASIL'EV, E. A. ROMANOVSKII, and G. F. TIMUSHEV

Institute of Nuclear Physics, Moscow State University

Submitted to JETP editor August 31, 1961

J. Exptl. Theoret. Phys. (U.S.S.R.) 42, 395-402 (February, 1962)

Inelastic scattering of 6.6-MeV protons leading to the excitation of the 3.352-, 3.733-, and 3.912-MeV levels in Ca^{40} and the 0.131-, 0.984-, 1.291-, 1.523-, and 1.885-MeV levels in Mn^{55} is investigated. It is shown that direct processes play a large part in these inelastic scattering reactions. The spins and parities of the three lowest Ca^{40} levels are 0^+, 3^-, and 2^+, respectively. Indications have been found that the 0.131-, 0.984-, 1.291-, and 1.885-MeV levels in Mn^{55} are collective, while the 1.523-MeV level is of single-particle character.

THE inelastic scattering of protons on Ca^{40} and Mn^{55} was investigated with a rotating magnetic analyzer. The proton beam was accelerated in the 120-cm cyclotron of the Institute of Nuclear Physics at Moscow State University. The experimental technique has been described in an earlier publication.[1] We measured the angular distributions of elastically scattered protons and proton groups corresponding to excited Ca^{40} levels at 3.352 ± 0.010, 3.733 ± 0.014, and 3.912 ± 0.015 MeV, and to excited Mn^{55} levels at 0.131 ± 0.007, 0.984 ± 0.005, 1.291 ± 0.010, 1.523 ± 0.007, and 1.885 ± 0.007 MeV. These levels are in good agreement with the results obtained by other investigators.[2,3]

Figure 1 shows the spectrum of particles scattered at $\vartheta_{lab} = 79°50'$. The target was a layer of metallic manganese deposited on a polystyrene backing. The thickness of the manganese layer corresponded to an energy loss of the order 15 keV for 6.6-MeV protons. The symbols of the chemical elements have been used to label the corresponding peaks of elastically scattered protons. Roman numerals have been used to label the peaks corresponding to protons scattered inelastically on Mn nuclei.

Figure 2 shows the angular dependence of the ratio between the differential elastic scattering cross section and the Rutherford cross section (in the c.m. system) for Ca^{40} and Mn^{55}. Curve 2 was borrowed from [4]. The figure shows that the cross section for elastic scattering on Ca^{40} increases greatly compared with the Rutherford cross section at large scattering angles; the changes are less pronounced for Mn^{55}. The cause of this difference appears to be the large contribution of elastic scattering through a compound nucleus in the case of Ca^{40} compared with a small
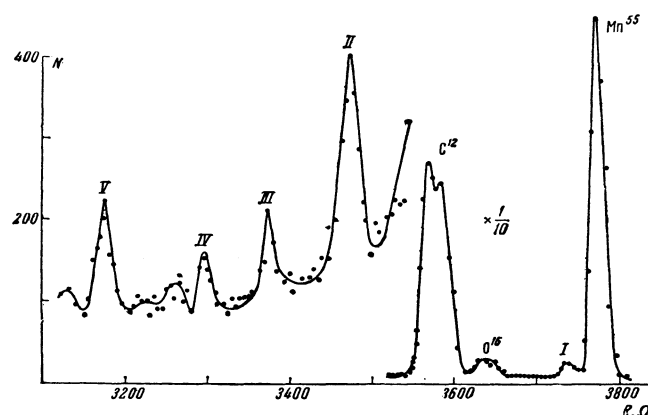

FIG. 1. Spectrum of protons scattered by a manganese target (with polystyrene backing) at $\vartheta_{lab} = 79°50'$. Abscissas represent resistances (in a resistance box) in the circuit of the analyzer-field meter. Ordinates are numbers of particles relative to a fixed number of counts of the beam-current integrator.

contribution in the case of Mn^{55}. The threshold of the (p, n) reaction for Ca^{40} is 15 MeV. Since Ca^{40} is a magic nucleus, the proton binding energy in the compound nucleus Sc^{41} has an extremely small value ~1.624 MeV.[5] There is therefore a high probability that only protons will be emitted from the compound nucleus, which has the excitation energy 8.2 MeV for $E_p = 6.6$ MeV. For Mn^{55} the (p, n) reaction threshold is 1.020 MeV and the (p, α) threshold is 2.568 MeV. Also, the proton binding energy in the compound nucleus Fe^{56} is 10.45 MeV, and the excitation energy of this compound nucleus is about 16 MeV for $E_p = 6.6$ MeV. Therefore the (p, n) reaction is most probable. The elastic cross section for proton scattering through a compound nucleus can be computed by analyzing the experimental data on inelastic proton scattering.

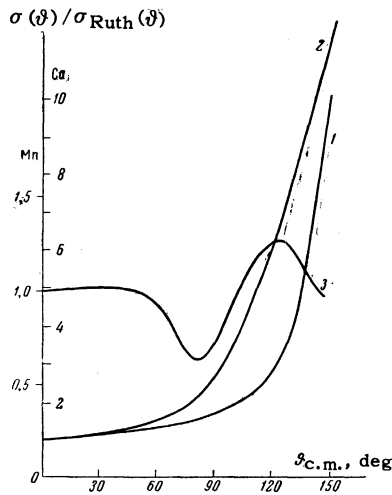Figures 3 and 4 show the angular distributions

$\sigma\,(\vartheta)\,/\sigma_{Ruth}\,(\vartheta)$

FIG. 2. Dependence of the ratio of the elastic scattering cross section to the Rutherford cross section on the scattering angle for Ca^{40} and Mn^{55}. Curves 1 and 2 — for Ca^{40} at E_p=6.6 MeV and 5.4 MeV, respectively; curve 3 — for Mn^{55} at E_p=6.6 MeV.

of protons associated with the Ca^{40} excitation energies 3.352, 3.733, and 3.912 MeV. Figures 5 and 6 show the angular distributions associated with the Mn^{55} excitation energies 0.131, 0.984, 1.291, 1.523, and 1.885 MeV. All angular distributions for Ca^{40} are asymmetric around 90°, with considerable
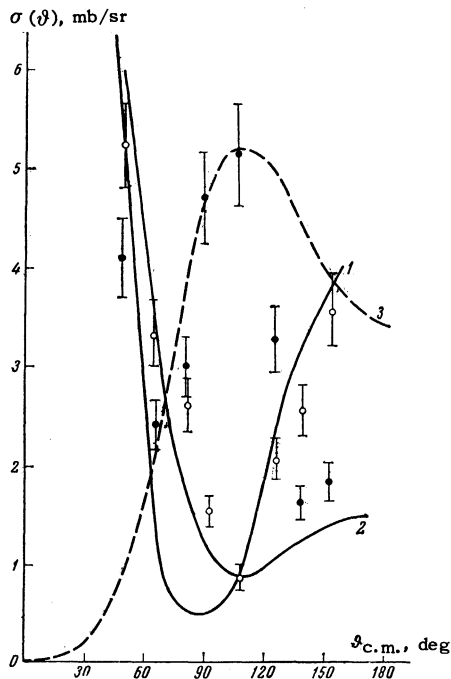
$\sigma\,(\vartheta)$, mb/sr

FIG. 3. Angular distribution of protons scattered from Ca^{40} excited to the levels 3.352 ± 0.010 MeV (o, continuous curves) and 3.733 ± 0.014 MeV (•, dashed curve). Curve 1 — calculated with distorted waves (L = 0); curve 2 — square of spherical Bessel function j_0^2 ($|k_i - k_f|$ R), R = 4.3 F; curve 3 — square of spherical Bessel function j_3^2 ($|k_i - k_f|$ R), R = 6 F.
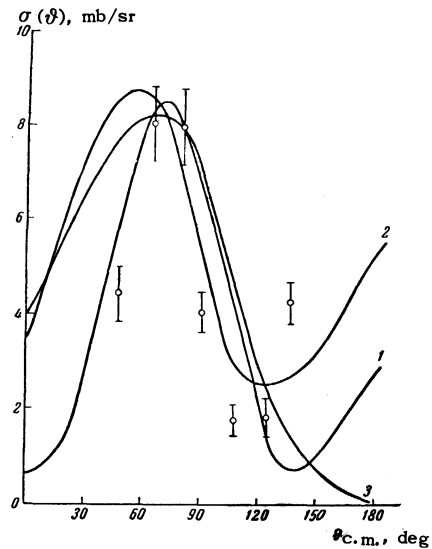
$\sigma\,(\vartheta)$, mb/sr

FIG. 4. Angular distribution of 6.6-MeV protons scattered by Ca^{40} with excitation energy 3.912 ±0.015 MeV. Curve 1 — calculated with distorted waves with L = 2, R = 1.2 A$^{\frac{1}{3}}$ F; curve 2 — same with L = 2, R = 1.5 A$^{\frac{1}{3}}$ F; curve 3 — square of spherical Bessel function j_2^2 ($|k_f - k_i|$ R), R = 6 F.

change from level to level. It should be noted that in these measurements we used a proton beam having a total energy spread ~45 keV, while the target thickness corresponded to ~20 keV loss. According to Gofman and Pasechnik,[6] in nuclei with A ~ 40 the mean level separation at excitation energy ~9 MeV is a few thousand electron volts, so that a large number of levels overlap in the compound nucleus. Consequently, the angular distribution of protons emitted by the compound nucleus should be either isotropic or symmetric around 90°.

In the case of proton scattering by Mn^{55} excited to 1.523 MeV (Fig. 6) the angular distribution was isotropic, in agreement with the statistical theory.
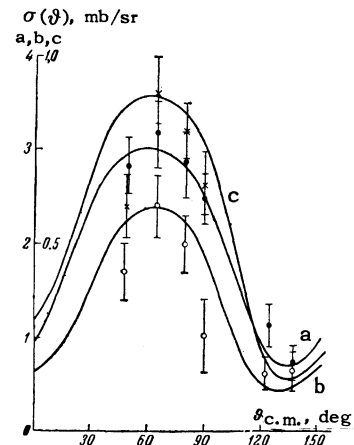
$\sigma\,(\vartheta)$, mb/sr
a,b,c

FIG. 5. Angular distribution of 6.6-MeV protons scattered by Mn^{55} with excitation energy 0.131 MeV (•, curve a), 0.984 MeV (o, curve b), and 129.1 MeV (×, curve c). The curves were calculated from Eq. (2).
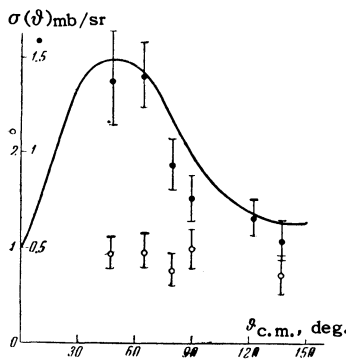
Fig. 6. Angular distribution of protons scattered by Mn^{55} with excitation energy 1.523 MeV (o) and 1.885 MeV (●). The curve was calculated from Eq. (2).

For all other investigated Mn^{55} levels the angular distributions were anisotropic and asymmetric around 90° with a maximum at $\vartheta_{c.m.}$ ~60°.

We conclude from the foregoing results that direct excitation processes play a large part in the inelastic scattering of protons on Ca^{40} and Mn^{55}. As a test of this hypothesis we compared the experimental angular distributions with predictions based on models of direct interactions in inelastic scattering. In these calculations it was assumed that the interaction of a proton with a Mn^{55} nucleus, leading to the excitation of four Mn^{55} states, is of collective character because of the collective nature of these levels. This hypothesis is based on the difficulties encountered when one attempts to use the shell model to account for the spins, quadrupole moments, and Coulomb excitation cross sections of the 0.131- and 0.984-MeV levels. For j-j coupling in the shell model the ground-state spin of an even-N odd-Z nucleus is the angular momentum j of the last incomplete shell.[7] (The $1f_{7/2}$ shell becomes occupied in nuclei with 20 < N < 28 or 20 < Z < 28.) We would therefore make the spin and parity assignment $\frac{7}{2}^-$ of the Mn^{55} ground state, although the experimental value is $\frac{5}{2}^-$.[8]

The existence of unusual coupling, leading to spin and parity $\frac{5}{2}^-$, is quite unexpected on the basis of elementary shell theory. The anomalous spin of the ground state could be accounted for by the mixing of proton configurations. Assuming the mixing of the configurations $(f_{7/2})^{-3}$, $(f_{7/2})^{-2}f_{5/2}^{-1}$, and $(f_{7/2})^{-2}f_{3/2}^{-1}$, Yanagawa[9] showed that the $\frac{5}{2}^-$ state has minimum energy, while the $\frac{7}{2}^-$ state lies 0.2 Mev above the ground state.

It is much more difficult to explain the large Mn^{55} quadrupole moment, $(0.4 \pm 0.2) \times 10^{-24}\,cm^{2}$[8] on the basis of the shell model. The calculated value is $0.04 \times 10^{-24}\,cm^2$. The large quadrupole moment indicates a nonspherical equilibrium shape of the Mn^{55} nucleus.

The ground-state properties of intermediate atoms including Mn^{55} were determined in [10] from the unified nuclear model.[11] This model leads to very good agreement between experiment and the calculated values of I, as well as of the magnetic and quadrupole moments.

The data on Coulomb excitation of the 0.131- and 0.984-MeV levels by protons[12] and α particles [13] indicate that the reduced probability of electric-quadrupole excitation of these levels is one order of magnitude greater than for single-particle levels.

Very little is known at present regarding the properties of excited states in the doubly magic nucleus Ca^{40}. For example, in the latest and most complete review by Gove,[14] which deals with the systematics of nuclear properties from O^{16} to Ca^{40}, for Ca^{40} only Braams'[2] values of the energy levels are given along with the spin and parity assignment 0^+ for the first Ca^{40} level. The inelastic scattering cross sections were calculated assuming both collective and single-particle characters for these excited states.

The experimental angular distributions were compared with those calculated from

$$d\sigma / d\Omega \sim j_l^2 (|\,k_i - k_f\,|\,R) \qquad (1)$$

(where k_i and k_f are the wave numbers of the incident and scattered protons, R is the interaction radius, l is the orbital quantum number, and j_l is the spherical Bessel function), and also with the inelastic scattering model of Rost and Austern,[15] based on the distorted-wave method. In the calculation of the matrix elements exact wave functions were used to describe the motion of the particle before and after the collision in an optical nuclear potential. The part of the optical potential associated with nuclear deformation was regarded as the perturbation causing the transition from the ground to the final state.

For quadrupole excitation (L = 2) the differential cross section is

$$\frac{d\sigma}{d\Omega} \sim \sum_{M=0,\,1,\,2} \varepsilon_M \left| \sum_{ll'} i^{l-l'}\,\sqrt{2l+1}\,\exp\left[i(\sigma_l + \sigma_{l'})\right] \right.$$

$$\left. \times f_l\,(\rho_i)\,f_{l'}\,(\rho_f)\,Y_{l'M}(\vartheta,\,0)\,C_{000}^{l'2l}C_{-M\,M0}^{l'2l} \right|^2. \qquad (2)$$

For a monopole transition (L = 0) we have

$$\frac{d\sigma}{d\Omega} \sim \left| \sum_{l=0}^{\infty} \sqrt{2l+1}\,\exp\,(2i\sigma_0)\,Y_{l0}\,(\vartheta,\,0)\,f_l\,(\rho_i)\,f_l\,(\rho_f) \right|^2. \qquad (3)$$

In Eqs. (2) and (3),

$$f_l\,(\rho) = \tfrac{1}{2}\,i\,[H_l^*\,(\rho) - \eta_l H_l\,(\rho)], \qquad (4)$$

$$H_l\,(\rho) = G_l\,(\rho) + iF_l\,(\rho),$$

where $\rho = kR$; $F_l(\rho)$ and $G_l(\rho)$ are the regular and irregular Coulomb wave functions tabulated in [16]; σ_l and η_l are the Coulomb and nuclear phase shifts, respectively; Y_{lM} is the l-th spherical harmonic; $\epsilon_M = 2 - \delta_{M0}$; $C_{\alpha\beta\gamma}^{abc}$ are Clebsch-Gordan coefficients.

For the sake of simplicity in calculations with (2) and (3) we assumed that the interaction potential for both elastically and inelastically scattered protons consists of a Coulomb potential and the potential of an interaction between a particle and an ideal solid sphere of radius R. On this basis the nuclear phase shift η_l can be calculated from

$$\eta_l = [G_l(\rho) - iF_l(\rho)] / [G_l(\rho) + iF_l(\rho)]. \qquad (5)$$

In the case of inelastic proton scattering on Ca^{40} with excitation of the first level (0^+) good agreement was obtained between experiment and Eq. (3). This is shown by curve 1 in Fig. 3, which also has a curve calculated from Eq. (1) for $l = 0$ and R = 4.3 F (curve 2). Curve 2 is seen to agree well with experiment only for small scattering angles.

The angular distributions for the 3.733- and 3.912-MeV levels differ in shape from that for the first excited level. Without changing our hypothesis regarding the character of the proton-nucleus interaction for the 3.912-MeV excitation energy, we used (2) to calculate the angular distributions shown in Fig. 4. Here for curve 1, $\rho_i = 2.2$ and $\rho_f = 1.4$, while for curve 2, $\rho_i = 3.0$ and $\rho_f = 1.9$. Curve 3 was calculated from (1) for $l = 2$ and R = 6 F. By comparing these curves with experiment we can arrive at some conclusion regarding the spin and parity of the 3.912-MeV level. According to the selection rules,[17]

$$I_i + I_f + 1 \geqslant L \geqslant |I_i + I_f + 1|_{min}, \qquad (6)$$
$$\pi_i \pi_f = (-1)^l,$$

where π is the parity, the spin and parity assignment of this level lies within the limits $1^+ \leq I_f^\pi \leq 3^+$.

The properties of the 3.9-MeV level of Ca^{40} have also been studied in [18], where a calcium target was irradiated with 5.7-MeV protons. A pair spectrometer was used to register 3.7- and 3.9-MeV γ rays. An electron-positron pair is emitted in the ground-state transition from the 3.3-MeV level. It was shown in [18] that emission from the 3.9-MeV level makes the principal contribution. A comparison of the measured and theoretical γ-ray angular distributions shows that best agreement is obtained if spin 2 is assigned to the 3.9-MeV level. Our data in conjunction with [18] thus indi-

cate that the 3.912-MeV level has spin 2 and positive parity.

It is seen from Fig. 3 that the maximum of the angular distribution for the 3.733-MeV level is shifted by about 40° with respect to the maximum for the 3.912-MeV level. The angular distribution for the 3.733-MeV level cannot be reconciled with the theoretical value for L = 2 by using any reasonable values of the parameters in (2). The curve in Fig. 3 calculated from (1) for $l = 3$ and R = 6 F can account for the location of the measured angular distribution maximum. For the 3.733-MeV level it follows from the selection rules that $1^- \leq I_f^\pi \leq 4^-$. From experiments on the inelastic scattering of 187-MeV electrons by Ca^{40}[19] it was concluded that this level has spin 3. In conjunction with our results we thus obtain the assignment 3^- for the 3.733-MeV level.

The sequence of assignments of the lowest Ca^{40} levels thus becomes 0^+, 3^-, 2^+. According to Gove,[14] the same sequence is observed for the 6.06-, 6.14- and 6.92-MeV levels of O^{16}. The high excitation energies of the 0^+ and 3^- levels of O^{16} and Ca^{40} indicate that these states cannot be simple surface vibrations, but must result from changes in the internal structure or density of the nuclei.[20] A possible explanation of the nature of spin-3 states in spherical nuclei can be found in [21]. The observed similarity between the properties of the lowest levels of Ca^{40} and O^{16} could be important for the theory of spherical nuclei with A ≥ 40.

For inelastic proton scattering on Mn^{55} good agreement was obtained between experiment and the theoretical angular distributions calculated from (2). The results are represented by the curves in Figs. 5 and 6. In the excitation of the 0.131-, 0.984-, 1.291-, and 1.885-MeV levels the angular momentum L = 0 is transferred; therefore, according to the selection rules, the spins and parities of these levels are contained within the limits $\frac{1}{2}^- \leq I^\pi \leq 11\frac{1}{2}^-$. Additional experimental data will have to be analyzed to establish the spins more precisely.

The 0.131-MeV level. The unique assignment of this level is $\frac{7}{2}^-$.[8]

The 0.984-MeV level. The scheme of the γ transitions from 0.984 MeV has been studied in [22,23]. According to Freeman[22] the intensity Y_{21} of the transition from this level to the first level is 95%, with $Y_{20} = 5\%$ for the ground-state transition. In [23] we find $Y_{21} = 93\%$, $Y_{20} = 7\%$ ($Y_{20}/Y_{21} = 0.08$).

We shall assume that the ground state and the 0.984- and 0.131-MeV levels belong to the same

rotational band. The ratio of the reduced probabilities B for γ transitions of identical multipolarity between an initial state I_2, K_2 and two final states I_1, K_1 and I_0, K_0 (where K is the projection of the spin on the nuclear axis of symmetry, and K_1 = K_2 = K_0 = I_0) is given by[11]

$$B(L,\ I_2 \to I_0)\,/\,B(L,\ I_2 \to I_1) = |\,C_{K_0 0 K}^{I_2 2 I_0}\,/\,C_{K 0 K}^{I_2 2 I_1}\,|^2. \tag{7}$$

In this equation L is the multipolarity of the transition, and $C_{\alpha\beta\gamma}^{abc}$ represents the Clebsch-Gordan coefficients. For E2 transitions (7) gives the intensity ratio $Y_{20}/Y_{21} = 0.33$ for these levels. This is close to the values 0.08 and 0.14 (the latter determined from Coulomb excitation experiments) if we assign $\frac{9}{2}^-$ to the 0.984-MeV level. The energy dependence of the (n, n'γ) cross section[23] is also in better agreement with the $\frac{9}{2}^-$ assignment, which is thus indicated by all the experimental data.

The 1.291-MeV level. The ratio $Y_{20}/Y_{21} = 0.14$ is given in [23]. Eq. (1) gives 0.33 for E2 transitions if $I^\pi = \frac{9}{2}^-$, and a zero value if $I^\pi = \frac{11}{2}^-$. The energy dependence of the (n, n'γ) reaction is in better agreement with the $\frac{11}{2}^-$ assignment.

The 1.523-MeV level. The ratio $Y_{20}/Y_{21} = 9$ is given in [23]. The value of this ratio obtained from formulas for single-particle transitions and the data on the energy dependence of the (n, n'γ) reaction are in best agreement with a $\frac{3}{2}^-$ assignment.

A comparison of our results with [23] indicates a single-particle character for the 1.523-MeV level. It is interesting that the separation between the $p_{3/2}$ and $f_{7/2}$ levels of Mn^{55} is comparable to the analogous separation in neighboring nuclei:[8]

Nucleus:	$_{20}Ca^{41}$	$_{21}V^{51}$	$_{24}Cr^{53}$	$_{22}Ti^{49}$	$_{27}Co^{59}$
ΔE, MeV:	1.950	0.928	0.970	1.380	1.289

The 1.885-MeV level. According to [23] the ratio Y_{20}/Y_{21} for this level is in the range 3.3 − 6.7. A computation of this ratio from (7) for E2 transitions favors the assignment $\frac{7}{2}^-$. The data on the (n, n'γ) reaction agree with $\frac{3}{2}^- \le I^\pi \le \frac{7}{2}^-$. The most probable spin of this level evidently is $\frac{7}{2}$ with negative parity.

The foregoing considerations indicate that both collective and single-particle excited states exist in Mn^{55}.

[1] Vasil'ev, Romanovskiĭ, and Timushev, JETP 40, 972 (1961), Soviet Phys. JETP 13, 678 (1961).

[2] C. M. Braams, Phys. Rev. 101, 1764 (1956).

[3] Mazari, Sperduto, and Buechner, Phys. Rev. 108, 103 (1957).

[4] Vanetsian, Klyucharov, Timoshevskiĭ, and Fedchenko, JETP 40, 1199 (1961), Soviet Phys. JETP 13, 842 (1961).

[5] H. E. Gove, Nuclear Reactions, Amsterdam, 1959.

[6] Yu. V. Gofman and M. V. Pasechnik, Trudy Vsesoyuznoĭ konferentsii po yadernym reaktsiyam pri malykh i srednikh energiyakh (Trans. All-Union Conference on Nuclear Reactions at Low and Medium Energies), November, 1957, AN SSSR, 1958, p. 234.

[7] M. Goeppert-Mayer and J. H. D. Jensen, Elementary Theory of Nuclear Shell Structure, (John Wiley and Sons, New York, 1955).

[8] B. S. Dzhelepov and L. K. Peker, Skhemy raspada radioaktivnykh yader (Decay Schemes of Radioactive Nuclei), AN SSSR, 1958.

[9] S. Yanagawa, J. Phys. Soc. Japan 14, 539 (1959).

[10] Val'ter, Zalyubovskiĭ, and Lutsik, Ukr. Fiz. Zh. 4, 705 (1959).

[11] S. G. Nilsson, Deformation of Atomic Nuclei, (Russ. Transl.) IIL, 1958.

[12] Mark, McClelland, and Goodman, Phys. Rev. 98, 1245 (1955).

[13] G. M. Temmer and N. P. Heidenburg, Phys. Rev. 96, 426 (1954).

[14] H. E. Gove, Proc. Intern. Conf. on Nuclear Structure, Kingston, 1960, p. 438.

[15] E. Rost and N. Austern, Phys. Rev. 120, 1375 (1960).

[16] Luk'yanov, Teplov, and Akimova, Tablitsa volnovykh kulonovskikh funktsiĭ (Table of Coulomb Wave Functions), AN SSSR, 1961.

[17] S. T. Butler, Nuclear Stripping Reactions, Horowitz Publications, Inc., Sydney, 1957 (Russ. Transl., IIL, 1960).

[18] Hirao, Okada, Miura, and Wakatsuki, J. Phys. Soc. Japan 13, 233 (1958).

[19] R. H. Helm, Phys. Rev. 104, 1466 (1956).

[20] A. M. Lane and E. D. Pendlebury, Nuclear Phys. 15, 39 (1960).

[21] Brown, Evans, and Thouless, Nuclear Phys. 24, 1 (1961).

[22] J. M. Freeman, Phil. Mag. 46, 12 (1955).

[23] Nath, Rothman, Van Patter, and Mandeville, Nuclear Phys. 13, 74 (1959).